

Electronic and geometric structure of the 3d-transition metal monocarbonyls MCO, M=Sc, Ti, V, and Cr

Constantine Koukounas, Stavros Kardahakis, and Aristides Mavridis^{a)}

Laboratory of Physical Chemistry, Department of Chemistry, National and Kapodistrian University of Athens, P.O. Box 64 004, 15710 Zografou, Athens, Greece

(Received 21 April 2005; accepted 17 May 2005; published online 25 August 2005)

The electronic and geometric structure of the 3d-transition metal monocarbonyls MCO, M=Sc, Ti, V, and Cr was investigated through coupled cluster (CC) and multireference variational methods (MRCI) combined with large basis sets. For the ground and a few low-lying excited states complete potential energy profiles were constructed at the CC-level of theory. The M–CO dissociation energies of the ground states $\tilde{X}^4\Sigma^-$, $\tilde{X}^5\Delta$, $\tilde{X}^6\Sigma^+$, and \tilde{X}^7A' are calculated to be 36, 27, 18, and 2 kcal/mol for ScCO, TiCO, VCO, and CrCO, with respect to Sc(⁴F), Ti(⁵F), V(⁶D), Cr(⁷S) + CO($X^1\Sigma^+$). The bonding is rather complicated and could be attributed mainly to π -conjugation effects between the M and CO π -electrons, along with weak σ -charge transfer from CO to M atoms. Almost in all cases the metal atoms appear to be slightly positively charged, at least according to the direction of the dipole moment vectors and the MRCI population densities. © 2005 American Institute of Physics. [DOI: 10.1063/1.1949199]

I. INTRODUCTION

The elucidation of the bonding mechanism between a first row transition metal (M) and carbon monoxide (CO) is of significant importance for both applied and academic reasons. On the practical side, the “unsaturated” monocarbonyls (MCO) can be considered as prototypical systems for the more complex polycarbonyls $[M(CO)_x]$ which are of wide interest in a variety of fields, such as organometallic chemistry, catalysis and surface chemistry.¹ Generally speaking, a relatively large number of experimental and theoretical studies has been published on the monocarbonyl MCO systems.

On the first four members of the MCO series (M=Sc, Ti, V, Cr), however, experimental information is close to none. A glance at Table I which summarizes all the experimental results available, is, indeed, convincing. With the exception of the MC–O stretching frequencies obtained in solid rare gas matrices (see footnotes of Table I), the only definitive data are those determining the ground states of ScCO (⁴ Σ) and VCO (⁶ Σ) obtained by electron spin resonance (ESR) spectroscopy.^{3,7} The dissociation energy of Ti–CO (40.4 kcal/mol) listed in Table I, is rather overestimated by about 30% (*vide infra*).

In Table II we have tabulated practically all theoretical studies published so far on the MCO molecules, M=Sc, Ti, V, and Cr. The size of the list is impressive but we cannot say the same thing on the consistency of the reported results. For instance, ground state binding energies of Sc–CO, Ti–CO, V–CO, and Cr–CO range from 26¹¹ to 50,¹⁸ 18¹³ to 45,¹⁸ 8¹³ to 33,¹⁷ and 0.5¹⁴ to 14²⁰ kcal/mol, respectively. Recall that the experimental value of the Cr–CO dissociation energy is less than 1.5 kcal/mol (Table I). Correspondingly, M–CO bond distances range from 2.07¹⁸–2.15,¹³ 1.98¹⁹–2.14,⁶

1.97¹⁷–2.09,¹³ and 2.07²⁰–2.35¹⁴ Å. We hasten to add though that the results listed on Table II were obtained through a plethora of *ab initio* and density functional methods and basis sets. Therefore, taking also into account the well recognized abstruseness of these molecular systems, this gamut of conflicting results is not entirely unexpected. Nevertheless the question remains as to the “usefulness” of all these numbers, namely, our ability to answer a question concerning, for instance a binding M–CO energy with a certainty of, say 10% or better.

Another open question is the conventional bonding scenario of the carbonyl to the metal atom, namely if the venerable Dewar–Chatt–Duncanson (DCD)²¹ mechanism (σ OC→M donation, π M↔CO back donation to the π^* -CO orbitals) is adequate.

In light of the above we have performed systematic all electron state-of-the-art *ab initio* calculations of the MCO (M=Sc, Ti, V, and Cr) molecules, employing coupled cluster (CC) single reference as well as variational multireference methods in conjunction with large basis sets. We have examined in a uniform way ground and low-lying excited states, constructing at the same time potential energy profiles at the CC-level of theory; we provide M–CO binding energies, geometries, energy separations, harmonic frequencies and dipole moments.

The paper is structured as follows: In Sec. II we give a qualitative, “chemically oriented” description of the bonding problem, while Sec. III outlines methods and technical details. Section IV refers to results and discussion and Sec. V is a broad summary of our findings and some final remarks.

II. PRELIMINARIES

The electronic configurations, terms and experimental energy separations of the ground and first excited states of the first four 3d-transition metal atoms, are²²

^{a)}Electronic mail: mavridis@chem.uoa.gr

TABLE I. Existing experimental data on the MCO molecules, M=Sc, Ti, V, and Cr.

Species	Ref./Year	State	D^a	$\omega(\text{MC-O})^b$
ScCO	2/1986 ^c			1950
	3/1989 ^d	$\bar{X}^4\Sigma$ $^4\Pi^e$		
TiCO	4/1999 ^f			1851.4/1834.2
	5/1988 ^g		40.4	
VCO	6/1999 ^h			1920.0/1887.8
	7/1986 ⁱ	$\bar{X}^6\Sigma^j$		
CrCO	6/1999 ^k			1930.6/1900.4
	2/1986 ^l			1977
	8/1997 ^m	“Septet”	<1.5	
	9/1997 ⁿ			1975.3
	10/2003 ^o			2018.4

^aDissociation energies M–CO in kcal/mol.^bMC–O stretching frequencies in cm⁻¹.^cTentative assignment obtained by IR spectroscopy in Ar matrices at 4 K.^dESR spectroscopy in Ar matrices at 4 K.^eIndications of a low-lying $^4\Pi$ state with an energy separation $T_e(^4\Pi \leftarrow \bar{X}^4\Sigma) \approx 500$ cm⁻¹.^fLaser-ablated generated Sc atoms reacting with CO₂ and isolated in Ne/Ar matrices.^gChemiluminescence emission spectroscopy on Ti(CO)_x, x=1,2.^hAs in (f) but Ti instead of Sc.ⁱESR spectroscopy in rare gas matrices, Ne, Ar, and Kr at 4 K.^jThe case that the ground state is of $^6A'$ symmetry is not ruled out.^kAs in (f) but V instead of Sc.^lIR spectroscopy in Ar matrices at 4 K.^mTime resolved single photon dissociation technique combined with detection of atomic fluorescence.ⁿLaser-ablated generated Cr atoms reacting with CO₂ and isolated in Ar matrices.^oSame as in (f) but Cr instead of Sc.

$$\text{Sc}[^2D(4s^23d^1), ^4F(4s^13d^2)]^4F \leftarrow ^2D = 1.427 \text{ eV},$$

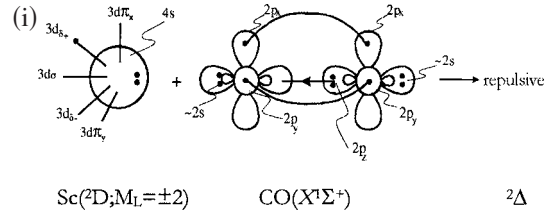
$$\text{Ti}[^3F(4s^23d^2), ^5F(4s^13d^3)]^5F \leftarrow ^3F = 0.806 \text{ eV},$$

$$\text{V}[^4F(4s^23d^3), ^6D(4s^13d^4)]^6D \leftarrow ^4F = 0.245 \text{ eV},$$

$$\text{Cr}[^7S(4s^13d^5), ^5S(4s^13d^5)]^5S \leftarrow ^7S = 0.941 \text{ eV}.$$

On the other hand, CO is an extremely strongly bound closed shell molecule ($D_0=255.78$ kcal/mol²³) characterized by a small static dipole moment ($\mu_e=0.1222D$),²³ whose negative end resides on the C-end of the CO molecule. Assuming a linear approach of CO from its C-end towards an M-metal atom, two things are already evident: First, the symmetry of the resulting M–CO states is dictated by the symmetry of the M atom projected axially, and second, *bona fide* bound states cannot be formed from the $4s^23d^q$ ($q=1,2,3$) ground state configurations of Sc, Ti, and V due to Pauli–Coulomb repulsion. The situation for Cr is a little bit different, its ground state configuration being $4s^13d^{q+1}$ ($q=4$), but in essence conforms to the same principle.

Taking as an example the $M_L=\pm 2$ component of the 2D ground state of the Sc atom, the following valence-bond–Lewis (vbL) diagram is self explanatory:



Obviously, repulsive $^2\Sigma^+$ and $^2\Pi$ states are also predicted for the $M_L=0, \pm 1$ vector components, respectively. As a matter of fact we dare say that the “repulsiveness” of the three doublets should increase from $^2\Pi$ to $^2\Delta$ to $^2\Sigma^+$ states. The same picture obtains for Ti, V, and Cr by singly occupying the empty nonbonding 3d-orbitals appropriately.

We can create “bonding conditions” by a $4s^23d^4 \rightarrow 4s^13d^{q+1}$ “promotion,” i.e., exciting the Sc, Ti, or V atoms to their first excited states 4F , 5F , and 6D , respectively. Taking again the Sc atom as an example, the $M_L=0, \pm 1, \pm 2$, and ± 3 components of the 4F term are

$$|0\rangle = \sqrt{\frac{4}{5}}|4s^13d\pi_x^13d\pi_y^1\rangle + \sqrt{\frac{1}{5}}|4s^13d^1_{\delta^+}3d^1_{\delta^-}\rangle, \quad (1)$$

$$|\pm 1\rangle_{B_1} = \sqrt{\frac{4}{10}}|4s^13d^1_{\sigma}3d\pi_x^1\rangle - \sqrt{\frac{3}{10}}|4s^13d\pi_x^13d^1_{\delta^+}\rangle + \sqrt{\frac{3}{10}}|4s^13d\pi_y^13d^1_{\delta^-}\rangle, \quad (2)$$

$$|\pm 2\rangle_{A_1} = |4s^13d^1_{\sigma}3d^1_{\delta^+}\rangle, \quad (3)$$

$$|\pm 3\rangle_{B_1} = \sqrt{\frac{1}{2}}|4s^13d\pi_x^13d^1_{\delta^+}\rangle + \sqrt{\frac{1}{2}}|4s^13d\pi_y^13d^1_{\delta^-}\rangle \quad (4)$$

giving rise to quartets of Σ^-, Π, Δ , and Φ molecular symmetry upon interaction with the ground $X^1\Sigma^+$ state of CO. Assuming that a most attractive interaction should be the one which diminishes the Pauli–Coulomb repulsion between the Sc $4s^1$ and the carbon lone pair of CO, while maximizing at the same time the conjugation (see below) with its π system, the best suited component for bonding of the Sc 4F is the $M_L=0$, does not include the d^1_{σ} rather “repulsive” distribution but includes the conjugation favorable $3d\pi_x^13d\pi_y^1$ one and with a very large coefficient $[(4/5)^{1/2}]$. In other words the bonding in the $^4\Sigma^-$ state should result from the interplay between a $(4s3d_{\sigma}4p_z)^1$ hybridization which will polarize the $4s^1$ Sc density to the back and away of the approaching carbon lone pair, and the $(3d\pi_x^1, 3d\pi_y^1) - (\pi_x^2, \pi_y^2)$ ScCO conjugation. The vbL diagrams (ii) and (iii) show separately these two “bonding” factors,

TABLE II. Existing theoretical data in ScCO, TiCO, VCO, and CrCO molecules. Adiabatic dissociation energies D_e (kcal/mol), bond distances r_e (Å), dipole moments μ (Debye), and energy separations T_e (cm^{-1}).

Species	Ref./year	State	D_e	r_e (M-CO)	r_e (MC-O)	μ	T_e	
ScCO	11/1986 ^a	$\tilde{X}^4\Sigma^-$	26.3			2.03	0.0	
		$^4\Pi$	26.1			2.59	~80	
	12/1989 ^b	$^4\Sigma^-$	24.3	2.12	1.183			
		$^4\Sigma^-$	37.7 ^c	2.12 ^b	1.183 ^b			
		$^2\Pi$	Unbound					
	13/1989 ^d	$\tilde{X}^4\Sigma^-$	28.6	2.153	1.167	4.09	0.0	
		$\tilde{X}^4\Sigma^-$ ^e	36.9	2.129	1.207	3.13	0.0	
		$\tilde{X}^4\Sigma^-$ ^f	39.9	2.107	1.209	3.80	0.0	
		$^4\Phi$ ^d		2.274	1.160	3.63	2742	
			$^4\Pi$ ^d		2.274 ^e	1.160 ^e	3.84	3710
	14/1992 ^h	$\tilde{X}^4\Sigma^-$	34.6	2.11	1.21		0.0	
	15/1995 ⁱ	“Quartet”	12.9	2.082	1.163			
	16/1995 ^j	$\tilde{a}^2\Sigma^+$	8.69	2.070	1.165		1469	
	4/1999 ^k	$\tilde{X}^4\Sigma^-$		2.075	1.181		0.0	
		$^2\Pi$		2.068	1.183		2553	
	17/2003 ^l	$\tilde{X}^4\Sigma^-$	29.7	2.076	1.179	3.41	0.0	
	18/2003 ^m	$\tilde{X}^4\Sigma^-$	49.7	2.070	1.166		0.0	
			$^2\Pi$	41.3	2.202	1.143		2938
	TiCO	13/1989 ⁿ	$\tilde{X}^5\Delta$	18.4	2.111	1.155	3.21	0.0
			$\tilde{X}^5\Delta^o$	27.7	2.070	1.196	2.54	0.0
$\tilde{X}^5\Delta^p$			30.2	2.064	1.196	3.10	0.0	
$\tilde{X}^5\Delta^q$			26.3	2.040	1.168	2.64	0.0	
$^3\Delta^n$				2.110	1.156	2.14	3629	
$^5\Pi^n$				2.264	1.145	1.68	5807	
$^1\Pi^n$				2.090 ^f	1.152 ^f		7178	
$^1\Gamma^n$				2.090 ^f	1.152 ^f		7662	
14/1992 ^h		$\tilde{X}^5\Delta$	22.0	2.05	1.20		0.0	
15/1995 ⁱ		“Quintet”	26.3	2.034	1.155		0.0	
16/1995 ^j		$\tilde{a}^3\Delta$	8.56	2.025	1.157		6226	
19/1998 ^s		“Quintet”	25.08	1.984	1.161	3.76	0.0	
6/1999 ^t		$\tilde{X}^5\Delta$		2.015/2.142	1.174/1.156		0.0	
17/2003 ^l		$\tilde{X}^5\Delta$	35.5	2.016	1.172	3.08	0.0	
18/2003 ^m		$\tilde{X}^5\Delta$	45.3	2.021	1.159		0.0	
		$^3\Delta$	28.0 ^u	1.924	1.171		6051	
VCO		13/1989 ^v	$\tilde{X}^6\Sigma^+$	8.1	2.094	1.142	2.07	0.0
	$\tilde{X}^6\Sigma^{+w}$		17.8	2.034	1.185	1.70	0.0	
	$\tilde{X}^6\Sigma^{+x}$		20.5	2.031	1.185	2.11	0.0	
	$^6\Delta^v$			2.183	1.139	0.36 ^y	2097	
		$^4\Pi^v$		2.008 ^z	1.173 ^z	4.70	4597	
		$^4\Phi^v$		2.008 ^z	1.173 ^z	4.60	4839	
	14/1992 ^h	$\tilde{X}^6\Sigma^+$	16.3	2.04	1.21		0.0	
	15/1995 ⁱ	“Sextet”	25.0	1.991	1.150		0.0	
	16/1995 ^j	$\tilde{a}^4\Delta$	Unbound ^{aa}	1.984	1.151		9199	
	6/1999 ^t	$\tilde{X}^6\Sigma^+$		1.967/1.996	1.168/1.150		0.0	
		$^4\Phi$		1.868/1.916	1.184/1.168		5281/4722	
	17/2003 ^l	$\tilde{X}^6\Sigma^+$	33.0	1.969	1.167	3.06	0.0	
	18/2003 ^{ab}	$\tilde{X}^6\Sigma^+$	26.6	1.994	1.150		0.0	
$^4\Delta$		13.8 ^{ac}	1.909	1.167		4477		
CrCO	14/1992 ^h	$\tilde{X}^7\Sigma^+$	0.48	~2.35	1.19		0.0	
	20/1993 ^{ad}	\tilde{X} -state	14.1 ^{ac}	2.070	1.162	0.87	0.0	
	15/1995 ^{i,af}	“Septet”	5.5	2.240	1.144		4477	
	16/1995 ^j	$\tilde{a}^5\Sigma^-$	23.2 ^{ag}	1.886	1.170		0.0	
	9/1997 ^{ah}	\tilde{X}^7A'		2.162	1.163		0.0	
	17/2003 ^l	\tilde{X}^7A'	9.0	2.156	1.161	0.87	0.0	
	10/2003 ^{ai}	\tilde{X}^7A'		2.142/2.216	1.162/1.146		0.0	

TABLE II. (Continued.)

Species	Ref./year	State	D_e	$r_e(\text{M-CO})$	$r_e(\text{MC-O})$	μ	T_e
	18/2003 ^{aj}	\tilde{X}^7A'	5.8	2.216	1.143		0.0

^aCISD+Q (Q=Davidson correction)/pseudopotential+[2s1p2d/Sc,2s2p/C,O] valence basis set.

^bBond distances at the MP2/[8s6p3d/Sc,6-31G*/C,O] level; D_e at a limited MRCISD including the 3s²3p⁶ “core” electrons/[10s10p6d2f/Sc,8s6p2d1f/C,8s7p2d1f/O] level.

^cPreviously calculated D_e +Silver–Davidson correction [Chem. Phys. Lett. **52**, 403 (1977)].

^d3 e⁻-MRCI/[8s6p4d/Sc,4s3p/C,O].

^e13 e⁻(=3+4+6)-MCPF (modified coupled pair functional).

^f21 e⁻[(3+8)+4+6]-(core)MCPF/[8s7p4d/Sc,4s3p/C,O].

^gSame geometry as in ⁴ Φ .

^hCISD+Q/[8s6p3d/Sc,5s3p/C,O].

ⁱDFT (B3LYP)/DZ basis; D_e 's with respect to ground state fragments, [Sc(*a*²D);Ti(*a*³F);V(*a*⁴F);Cr(*a*⁷S)]+CO(*X*¹ Σ^+) (*vide infra*).

^jDFT (B3LYP)/DZ basis (?).

^kDFT (BP86)/[8s6p3d/Sc,6-311+G*/C,O].

^lDFT (BPW91)/[6-311+G*].

^mDFT (B3LYP)/[6-311G(2d)/Sc,6-311G(2d)/C,O]; D_e of the ² Π state calculated with respect to Sc(*a*⁴F)+CO(*X*¹ Σ^+).

ⁿ4 e⁻-MRCI/[8s6p4d/Ti,4s3p/C,O].

^o14 e⁻(=4+4+6)-MCPF.

^p22 e⁻[(4+8)+4+6]-(core)MCPF/[8s7p4d/Ti,4s3p/C,O].

^q14 e⁻-MCPF/[ANO-6s4p3d2f/Ti,4s3p2d1f/C,O].

^rUnoptimized bond lengths.

^sDFT (B3PW91)/[6-311G(dp)]. These authors use a variety of functionals besides the B3PW91, namely, B3LYP, PW91, BLYP, and BP86 with dramatically different results.

^tDFT (BP86/B3LYP)/[8s6p3d/Ti,6-311+G*/C,O].

^u D_e with respect to Ti(*a*⁵F)+CO(*X*¹ Σ^+).

^v5 e⁻-MRCI/[8s6p4d/v,4s3p/C,O].

^w15 e⁻(=5+4+6)-MCPF.

^x23 e⁻[(5+8)+4+6]-(core)MCPF/[8s7p4d/Ti,4s3p/C,O].

^yThe metal end of VCO is negatively charged.

^zGeometries optimized at the 5e⁻-CASSCF level on the same state.

^{aa}According to our calculations this is a volcaniclike state, therefore the numerical results rather refer to the local minimum.

^{ab}DFT (B3LYP)/[TZV/v,6-311+G(2d)/C,O].

^{ac} D_e with respect to V(*a*⁶D)+CO(*X*¹ Σ^+).

^{ad}DFT (BP/VWN). Although the author does not tag the \tilde{X} state, we presume that he refers to ⁷A'; $\angle\text{CrCO}$ angle $\approx 140^\circ$.

^{ae}Despite this D_e value (D_0 +BSSE correction=12.4 kcal/mol), the author suggests that CrCO can be unbound.

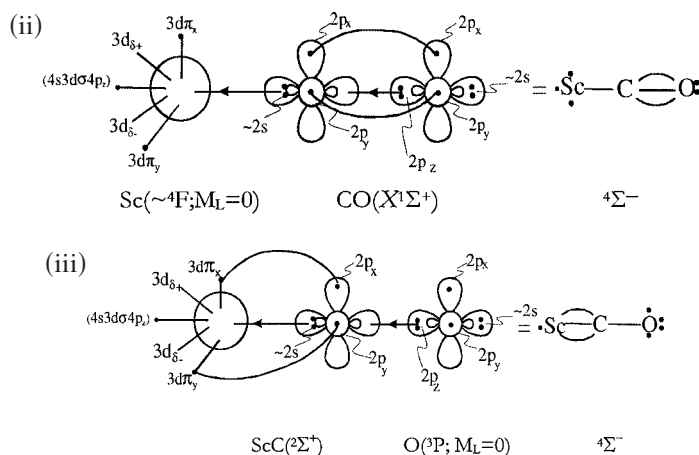
^{af} $\angle\text{CrCO}=135.2^\circ$.

^{ag} D_e with respect to Cr(3d⁴4s²; *a*⁵D)+CO(*X*¹ Σ^+), but this should be a ⁵ Σ^+ state and not a ⁵ Σ^- .

^{ah}DFT (LDA/BP); $\angle\text{CrCO}=137.5^\circ$; $\omega(\text{CrC-O stretch})=1913.9\text{ cm}^{-1}$.

^{ai}DFT (BP86/B3LYP)/[8s6p3d/Cr,6-311+G*/C,O]; $\angle\text{CrCO}=139.7^\circ/137.4^\circ$; $\omega(\text{CrC-O stretch})=1928.9/2015\text{ cm}^{-1}$.

^{aj}DFT (B3LYP)/(Stuttgart pseudopotential for the 1s²2s²2p⁶e⁻+ [6s5p3d1f/Cr,6-311+G(2d)/C,O]; $\angle\text{CrCO}=137.2^\circ$.

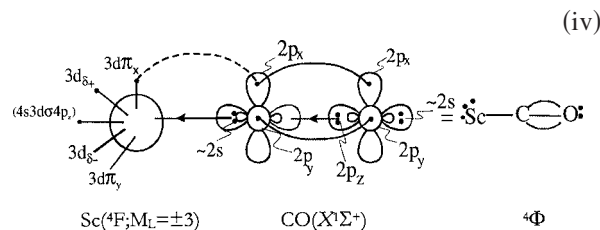


Scheme (iii) clarifies the meaning we ascribe to the word “conjugation,” namely, the spin coupling of the six π -electrons into a triplet. Incidentally, Scheme (iii) suggests that the formation of MCO molecules could have been ex-

amined from the MC+O perspective. Knowing by now the detailed electronic structure of the first four 3d-transition metal carbides,²⁴ this is a quite interesting and complementary approach. However, considering the “sturdiness” of the

CO molecule, the M+CO channel is certainly the most natural approach from a chemical point of view.

Following the same line of thought we predict two close in energy ScCO bound states of $^4\Pi$ and $^4\Phi$ symmetries but certainly higher than the $^4\Sigma^-$ state. As a matter of fact the $^4\Pi$ should be located above the $^4\Phi$ state albeit close, because of the $(4/10)^{1/2}$ “repulsive,” nonamenable to bonding, configuration [Eq. (2)]. Graphically, the bonding of the $^4\Phi$ ScCO state is shown in Scheme (iv) (B_1 component).



The limited conjugation in the $^4\Phi$ (and $^4\Pi$) states as contrasted to the $^4\Sigma^-$ state, namely $3d\pi_x - \pi_x^2$ versus $(3d\pi_x^1, 3d\pi_y^1) - (\pi_x^2, \pi_y^2)$, respectively, suggests a shorter Sc–CO bond length in the latter as compared to the former. Or, that the $^4\Sigma^-$ Sc–CO interaction acquires features of triple bond character, as opposed to double bond in $^4\Phi$ and $^4\Pi$ states; see Schemes (iii) and (iv). Finally, and in the light of the above, the $^4\Delta$ ScCO state ($M_L = \pm 2$) should be repulsive or van der Waals bound.

We recapitulate our thoughts on the Sc· · CO interaction.

- The ground state of ScCO is of $^4\Sigma^-$ symmetry.
- States $^4\Pi$ and $^4\Phi$ are bound with similar bonding character, but the $^4\Pi$ should be higher in energy due to the “repulsive” $(4/10)^{1/2}$ configuration of the $M_L = \pm 1$ component of the Sc 4F term. Therefore, the energy ordering of the four quartets should be $\tilde{X}^4\Sigma^- < ^4\Phi \approx ^4\Pi < ^4\Delta$ (repulsive).
- The Sc–CO bond distance of the $^4\Pi$ and $^4\Phi$ states should be considerably larger than in the $^4\Sigma^-$ state due to the increased conjugation in the latter as compared to the former states.
- By the same reasoning as in (c), upon formation of the ScCO molecule in the three bound quartets the Sc–O bond distance should increase as compared to the free CO ($X^1\Sigma^+$). The effect is expected to be more pronounced where the conjugation is maximum, i.e., in the $\tilde{X}^4\Sigma^-$ state.
- The “driving force” of the bonding process is caused by the synergism of the $M \curvearrowright \text{CO } \pi-$ and $\text{Sc} \leftarrow \text{CO } \sigma-$ interactions.

Our calculations completely vindicate the analysis above and the ensuing predictions.

Mutatis-mutandis the same conceptual line can be followed for the understanding of the electronic structure and bond formation of TiCO and VCO species.

III. TECHNICAL DETAILS

The ANO (atomic natural orbital) Gaussian basis sets $21s16p9d6f4g$ (Sc, Ti) and $20s15p10d6f4g$ (V, Cr) of

Bauschlicher²⁵ were used through all our calculations. For the light atoms the Dunning’s²⁶ correlation consistent basis sets of quadruple-zeta quality augmented with a series of diffuse functions, aug-cc-pVQZ = $13s7p4d3f2g$ (AQZ), were employed. Both sets were generally contracted to $[7s6p4d3f2g/M \ 6s5p4d3f2g/C,O]$ amounting to 244 spherical Gaussians.

The MCO (M=Sc, Ti, V, Cr) molecules are in general multireference in character with a relatively large number of “active” (valence) electrons (13, 14, 15, 16). While there is no doubt that the best calculational approach for an in depth description examining both channels M+CO and MC+O is the complete active space self-consistent field (CASSCF)+single+double+... replacements(CASSCF+1+2+...) method, even truncating the series at the CASSCF+1+2(=MRCI) level, the calculations are very time consuming. In addition, as the number of active electrons increases, size nonextensivity errors can corrode substantially the quality of the MRCI calculations. Since presently we only examine the M+CO→MCO channel and because of the specific type of the M–CO bond (see Sec. II), the single reference coupled-cluster CCSD(T) approach can be used even for the construction of potential energy M–CO curves. Of course, the CC-method is at its best when dealing with single reference states, which is (accidentally) the present case for many MCO states. Therefore the following strategy was picked.

Almost all of our M–CO PECs were constructed at the coupled cluster+ singles+doubles+perturbatively connected triples using restricted Hartree–Fock orbitals (=RCCSD(T)) level of theory. We also performed RCCSD(T) calculations limited around equilibrium distances including the $3s^23p^6$ semicore electrons of the M atoms [C-RCCSD(T)]. At the C-RCCSD(T)/ANO+AQZ level scalar relativistic effects were taken into account via the Douglas–Kroll–Hess (DKH) approximation.²⁷

For reasons of comparison and because of inaccessibility of certain states via the RCCSD(T) single reference approach, and for obtaining reliable population distributions, we have also performed MRCI calculations around equilibrium geometries using a limited reference CASSCF space constructed by allotting the 3, 4, 5, and 6 valence electrons of the Sc, Ti, V, and Cr atoms, respectively, to the six $4s3d$ M orbitals. All our CASSCF wave functions obey axial symmetry conditions. Note that in the MRCI calculations the basis sets on C and O are that of plain quadruple quality, i.e., the diffuse functions were removed ($[5s4p3d2f1g]_{C,O} = \text{cc-pVQZ}$). The single and double excitations out of the CASSCF reference space include, of course, all valence electrons of the MCO systems, i.e., 13, 14, 15, and 16 for ScCO, TiCO, VCO, and CrCO, respectively. The internally contracted MRCI spaces range from about 500 000 (ScCO, $\tilde{X}^4\Sigma^-$) to 1 200 000 (TiCO, $^3\Sigma^-$) configuration functions. For the MRCI calculations size nonextensivity effects which grow larger as we move from ScCO to CrCO, were ameliorated by using the super-molecule approach in calculating dissociation energies and the multireference Davidson correction (Q) for missing higher excitations. For the same reason we also performed multireference averaged coupled pair

functional (MRACPF) calculations, perhaps the most sophisticated method for confronting size nonextensivity problems.²⁸ However, because of the arbitrariness of the functional used, ACPF results should be considered with caution. Finally, basis set superposition errors (BSSE) were not taken into account, judging that BSSE effects are not significant as compared to all other approximations and/or omissions entailed in the present work.

Almost all our calculations were performed with the MOLPRO 2002.6 suite of codes;²⁹ certain specific results were obtained using the ACES II package.³⁰

IV. RESULTS AND DISCUSSION

Table III gives a complete view of all our results on the MCO series, M=Sc, Ti, V, and Cr; corresponding potential energy M–CO curves (PEC) at the RCCSD(T)/AQZ level are displayed in Figs. 1–4. Complete geometry optimization around equilibrium showed that all bound MCO states are linear.

A. ScCO

At the CCSD(T)/AQZ level of theory, the $X^1\Sigma^+$ state of the free CO is described well enough according to calculated values of its standard molecular parameters (experimental results in parenthesis²³): $D_e=256.5(258.9)$ kcal/mol, $r_e=1.1319(1.1283)$ Å, $\omega_e=2159(2169.8)$ cm⁻¹, and $\mu_e=0.12(0.1222)$ D.

For the ScCO we examined four quartets ($^4\Sigma^-, ^4\Pi, ^4\Delta, ^4\Phi$), and three doublets ($^2\Sigma^+, ^2\Pi, ^2\Delta$). Figure 1 shows PECs of Σ^-, Φ , and Δ quartets and the Σ^+, Π , and Δ doublets at the RCCSD(T)/AQZ level. As was explained before, some of the states (here the $^4\Pi$) are inaccessible at the single reference CC-level, therefore, we were also obliged to examine all four quartets correlating to $\text{Sc}(^4F)+\text{CO}(X^1\Sigma^+)$ using the MRCI method.

As was foreseen in Sec. II the three doublets emanating from $\text{Sc}(^2D)+\text{CO}$ are clearly repulsive, the “most” repulsive being the $^2\Sigma^+$ state. The $^2\Pi$ PEC shows a hump at about 2.65 Å, followed by a shallow well the depth of which is 640 cm⁻¹(=1.83 kcal/mol) from the hump’s maximum (2.634 Å), but 2.38 kcal/mol above the asymptotic ground state products at the RCCSD(T) level. The minimum is rather due to the slight hybridization of the $4s^2$ with the empty $3d\sigma$ orbital, but mainly to the incipient conjugation of the $3d\pi_x^1$ (or $3d\pi_y^1$) with the π_x (or π_y) system of the approaching CO moiety.

The first bound state of ScCO is of $^4\Sigma^-$ symmetry correlating to $\text{Sc}(^4F)+\text{CO}(X^1\Sigma^+)$. The binding energy with respect to adiabatic fragments is $D_e=37.6(40.0)[36.9]$ kcal/mol at the RCCSD(T) (C-RCCSD(T)) [C-RCCSD(T)+scalar relativistic corrections (DKH)] level of theory. Correcting for the (harmonic) zero point energy (ZPE) we get $D_0=36.5$ (38.9) kcal/mol; assuming that the relativistic effects do not influence the ZPE value, the C-RCCSD(T)+DKH is $D_0=35.8$ kcal/mol (see Table III). It is interesting though that the energy of the $^4\Sigma^-$ state+ZPE is 1.2 kcal/mol *above* the total energy of the ground state fragments at the RCCSD(T) level, but *lower (higher)* by 4.3(0.2) kcal/mol at the C-RCCSD(T) (+DKH) level. However, these differences are also related to the calculated $\text{Sc}(^4F\leftarrow^2D)$ splitting. The corresponding numbers are 13 188 (12 111) [12 592] cm⁻¹ as contrasted to the experimental²² value of 11 500 cm⁻¹. Considering that a parallel shift of the whole $^4\Sigma^-$ potential curve to match the experimental $^4F\leftarrow^2D$ separation is realistic in all three methods above, the total energy of the $^4\Sigma^-$ state is *lower* than the asymptotic fragments by 4.7 (7.1) [4.0] kcal/mol. Therefore the $^4\Sigma^-$ symmetry represents the true ground state of ScCO, albeit very close to the asymptotic ground state fragments, $\text{Sc}(^2D)+\text{CO}$.

Table III also lists multireference results and as expected binding energies are considerably smaller as compared to the CC values due to severe nonextensivity problems, particularly at the MRCI level.

The bonding in the $\tilde{X}^4\Sigma^-$ state of ScCO has been qualitatively described in Sec. II; our numbers are in accordance with these ideas. Due to the generally weak binding for all states in the MCO series, the wave functions at equilibrium can be described fairly well by the antisymmetrized product of the two fragments at infinity, i.e., $\psi(\text{MCO})=\hat{A}\psi(\text{M})*\psi(\text{CO})$, where $\psi(\text{CO})=|1\sigma^22\sigma^23\sigma^21\pi_x^21\pi_y^2\rangle$ counting the valence electrons only. Indeed, the leading equilibrium MRCI configurations of the ScCO $^4\Sigma^-$ state are

$$\begin{aligned} |\tilde{X}^4\Sigma^- \rangle &\approx |1\sigma^22\sigma^23\sigma^21\pi_x^21\pi_y^2[(0.94)4\sigma^12\pi_x^12\pi_y^1 \\ &\quad + (0.09)4\sigma^11\delta_x^11\delta_y^1] \rangle \\ &\approx \hat{A}\psi(\text{CO}) * \psi(\text{Sc}, ^4F; M_L = 0). \end{aligned}$$

Observe that upon bonding the $(4/5)^{1/2}(=0.89)$, $(1/5)^{1/2}(=0.45)$ coefficients of the free $\text{Sc}(^4F; M_L=0)$, increase (decrease) variationally to 0.94 (0.09), resulting to an adequately single reference description of the $\tilde{X}^4\Sigma^-$ state, thus ensuring the credibility of the CC-calculations.

The MRCI equilibrium (r_e) atomic populations as well as those of the asymptotic fragments ($r_\infty, \text{Sc}+\text{free CO}$), are as follows:

$$\begin{aligned} r_e: &4s^{0.85}3d_{z^2}^{0.15}4p_z^{0.29}4p_x^{0.06}4p_y^{0.06}3d_{xz}^{0.69}3d_{yz}^{0.69}3d_{\delta z}^{0.02} / \text{Sc}2s^{1.45}2p_z^{0.97}2p_x^{0.66}2p_y^{0.66}3d_{xz}^{0.06}3d_{yz}^{0.06} / \text{C}2s^{1.78}2p_z^{1.41}2p_x^{1.48}2p_y^{1.48} / \text{O} \\ r_\infty: &4s^{1.00}3d_{z^2}^{0.0}3d_{x^2-y^2}^{0.18}3d_{xy}^{0.18}3d_{xz}^{0.82}3d_{yz}^{0.82} / \text{Sc}2s^{1.82}2p_z^{0.93}2p_x^{0.50}2p_y^{0.50}3d_{xz}^{0.05}3d_{yz}^{0.05} / \text{C}2s^{1.73}2p_z^{1.43}2p_x^{1.43}2p_y^{1.43} / \text{O} \end{aligned}$$

TABLE III. Total energies E (hartree), dissociation energies D_e, D_0 (kcal/mol), equilibrium bond distances r_{M-CO} and r_{M-C-O} (Å), energy separations from the \bar{X} state T_e (cm⁻¹), harmonic frequencies $\omega_{1,2}, \omega_3, \omega_4$ (cm⁻¹), and dipole moments μ (D) of all MCO species and states presently studied, M=Sc, Ti, V, and Cr.

Method	$-E$	D_e	D_0^a	r_{M-CO}	r_{M-C-O}	T_e	$\omega_{1,2}$	ω_3	ω_4^b	$\langle \mu \rangle / \mu_{FF}^c$
ScCO										
$\bar{X}^4\Sigma^-$										
RCCSD(T)	872.96953	37.6	36.5	2.120	1.169	0.0	297	412	1890	/-3.34
C-RCCSD(T) ^d	873.26723	40.0	38.9	2.077	1.167	0.0	300	426	1877	/-3.37
C-RCCSD(T)+DKH ^e	876.92528	36.9		2.080	1.168	0.0				
MRCI	872.93840	24.1		2.101	1.145	0.0				-2.01/-2.44
MRCI+Q ^f	872.99364	30.3		2.099	1.159	0.0				/-2.24
ACPF	872.99869	32.9		2.127	1.161	0.0				-2.84/-2.80
Expt. ^g									1851/1834	
$\bar{a}^2\Pi$										
RCCSD(T)	872.96583	-2.38		2.211	1.149	812				/+0.20
C-RCCSD(T) ^d	873.26182	-2.00		2.175	1.147	1188				/0.0
$\bar{A}^4\Phi$										
RCCSD(T)	872.95373	27.7	26.8	2.266	1.163	3468	255	368	1896	/-2.78
C-RCCSD(T) ^d	873.24932	28.8		2.221	1.162	3932				/-2.71
C-RCCSD(T)+DKH ^e	876.9079	26.0		2.221	1.162	3812				
MRCI	872.93481	22.2		2.249	1.146	788				-2.58/-2.59
MRCI+Q ^f	872.98320	23.9		2.265	1.154	2291				/-2.44
ACPF	872.98122	22.5		2.264	1.150	3836				-1.87/-2.19
$\bar{B}^4\Pi$										
MRCI	872.93041	19.6		2.250	1.150	1753				-2.68/-2.85
MRCI+Q ^f	872.97907	21.6		2.247	1.158	3197				/-2.69
ACPF	872.97657	19.7		2.266	1.152	4855				-2.12/-2.29
Expt. ^h						~500				
TiCO										
$\bar{X}^5\Delta$										
RCCSD(T)	961.66496	27.5	26.4	2.059	1.160	0.0	285	415	1944	/-2.43
C-RCCSD(T) ^d	961.99113	29.5		2.033	1.158	0.0				/-2.37
C-RCCSD(T)+DKH ^e	966.44052	27.7		2.033	1.158	0.0				
MRCI	961.58573	14.5		2.077	1.135	0.0				+0.27/-0.92
MRCI+Q ^f	961.63731	20.7		2.057	1.150	0.0				/-1.73
ACPF	961.64428	25.4		2.099	1.152	0.0				-2.15/-1.70
Expt.			~40.4 ⁱ						1920/1888 ^j	
$\bar{a}^3\Delta$										
MRCI	961.56861	-8.2/25.3 ^k		2.068	1.136	3757				+0.31/-0.28
MRCI+Q ^f	961.62248	-4.9/28.3 ^k		2.057	1.151	3254				/-1.00
ACPF	961.62808	-3.7		2.088	1.153	3554				-1.02
$\bar{b}^3\Sigma^-$										
RCCSD(T)	961.64834	-4.2		2.132	1.137	3647				/+1.17
MRCI	961.55848	-12.0		2.133	1.117	5981				+1.52/+1.65
MRCI+Q ^f	961.61686	-7.7		2.068	1.134	4487				/+0.31
ACPF	961.62357	-6.0		2.063	1.140	4545				+0.55
$\bar{A}^5\Phi$										
RCCSD(T)	961.63457	8.4	7.7	2.233	1.152	6669	179	342	1957	
C-RCCSD(T) ^d	961.95760	8.4		2.209	1.149	7359				
C-RCCSD(T)+DKH ^e	966.40766	7.1		2.209	1.149	7212				
MRCI	961.56939	4.6		2.232	1.137	3585				-0.92/-0.37
MRCI+Q ^f	961.61427	6.5		2.226	1.145	5055				/-0.20
ACPF	961.61557	7.4		2.253	1.141	6300				+0.66
$\bar{B}^5\Pi$										
MRCI	961.56469	1.8		2.230	1.141	4618				-1.07
MRCI+Q ^f	961.60979	3.8		2.224	1.148	6040				/-0.35
ACPF	961.61081	4.6		2.255	1.141	7346				+0.32
$\bar{C}^5\Sigma^-$										
MRCI	961.55116	-6.5								
MRCI+Q ^f	961.60200	-0.67								
ACPF	961.60989	4.5		2.083	1.155	7546				+0.04/-0.86
$\bar{c}^3\Gamma$										
MRCI	961.55148			2.042	1.144	7517				-0.58/-2.14
MRCI+Q ^f	961.61037			2.038	1.159	5913				/-2.81

TABLE III. (Continued.)

Method	$-E$	D_e	D_0^a	r_{M-CO}	r_{MC-O}	T_e	$\omega_{1,2}$	ω_3	ω_4^b	$\langle \mu \rangle / \mu_{FF}^c$
VCO										
$\tilde{X}^6\Sigma^+$										
RCCSD(T)	1056.17504	18.1	17.0	2.012	1.150	0.0	276	388	1979	/-1.94
C-RCCSD(T) ^d	1056.52338	20.9		1.995	1.149	0.0				/-1.79
C-RCCSD(T)+DKH ^e	1061.88746	19.3		1.996	1.149	0.0				
MRCI	1056.09087	6.1		2.159	1.119	0.0				+2.23/+1.50
MRCI+Q ^f	1056.14380	10.4		2.087	1.134					/+0.48
Expt. ^j									1931/1904	
$\tilde{A}^6\Delta$										
RCCSD(T)	1056.16180	9.8		2.107	1.145	2906	100	328	2025	/+1.19
C-RCCSD(T) ^d	1056.50820	11.3		2.098	1.143	3333				/+1.44
MRCI	1056.08228	0.48		2.196	1.120	1887				+3.11
MRCI+Q ^f	1056.13450	4.4		2.126	1.134	2042				/+1.92
$\tilde{a}^4\Delta$										
RCCSD(T)	1056.15836	0.8		2.051	1.135	3661				
$\tilde{B}^6\Pi$										
RCCSD(T)	1056.14910	1.81		2.236	1.14	5693				
C-RCCSD(T) ^d	1056.4953	3.3		2.221	1.14	6163				
CrCO										
$\tilde{X}^7A'^1$										
RCCSD(T)	1156.65682	1.06		2.266	1.135	0.0				
C-RCCSD(T) ^d	1157.01917	3.72		2.185	1.136	0.0				
C-RCCSD(T)+DKH ^e	1163.43596	2.1								
Expt.			<1.5 ^m						2018 ⁿ /1975 ^o	
$\tilde{a}^5\Sigma^+$										
MRCI	1156.55478	3.9		2.178	1.113					+3.78/+3.15
MRCI+Q ^f	1156.61144	7.1		2.095	1.124					/+2.57
ACPF	1156.61842	9.2		2.174	1.128					+2.49/+2.29
MRCI+DKH ^e	1162.92041	5.7		2.178	1.113					
C-MRCI ^d	1156.46755	6.3		2.166	1.109					+3.81/+3.20
C-MRCI+Q ^f	1156.47379	9.7		2.058	1.120					/+2.52
$\tilde{A}^7\Pi^{pp}$										
RCCSD(T)	1156.62016	43.5		2.016	1.161	8046	373	507	1891	/-4.35
C-RCCSD(T) ^d	1156.98076	48.4		1.990	1.160	8432				/-3.94
MRCI	1156.53340	31.2		1.982	1.143					-2.82/-5.85
MRCI+Q ^f	1156.58929	36.1		1.946	1.157					
C-MRCI ^d	1156.82573	32.1		1.972	1.140					-2.87/-5.79
C-MRCI+Q ^f	1156.92704	38.3		1.933	1.154					

^a $D_0 = D_e - ZPE$.^b $\omega_4 = MC-O$ stretching. All frequencies were calculated using a triple-zeta cc-basis set on C and O.^c $\langle \mu \rangle$ calculated as expectation value, μ_{FF} calculated by the finite field approach; negative signs refer to M^+-CO^- polarity.^dThe $3s^23p^6$ semicore M electrons included.^eDouglas-Kroll-Hess scalar relativistic corrections.^fQ=Davidson correction^gReference 4.^hReference 3.ⁱReference 5.^jReference 6.^kWith respect to diabatic fragments $Ti(b^3F)+CO(X^1\Sigma^+)$.^l $\angle CrCO \approx 154^\circ$; barrier to linearity = $75 \text{ cm}^{-1}(^7\Sigma^+)$.^mReference 8.ⁿReference 10.^oReference 9.^pA set of $4p$ Cr orbitals has been included in the CASSCF procedure.

From the population densities above it is clear that the *in situ* Sc atom gains about $0.3 e^-$ through the σ -frame, with a concomitant loss of $2.0 - 2 * (0.69 + 0.06) = 0.5 e^-$ through the double π -conjugated system. In total, the charge distribution of the \tilde{X} -state of ScCO appears to be $Sc^{+0.15} - C^{+0.06} - O^{-0.21}$, or that about $0.15 e^-$ are transferred to CO upon bonding to the metal.

Concerning now the geometry of the $\tilde{X}^4\Sigma^-$ with respect to the $^4\Phi$ and $^4\Pi$ states and the bond length of the free CO, we observe that on going from the $\tilde{X}^4\Sigma^-$ to the $^4\Phi$ and $^4\Pi$ states the Sc-CO bond distance increases by 0.17 and 0.15 Å, respectively at the MRCI+Q level. A similar increase is observed between the $\tilde{X}^4\Sigma^-$ and $^4\Phi$ states, 0.14 Å at the

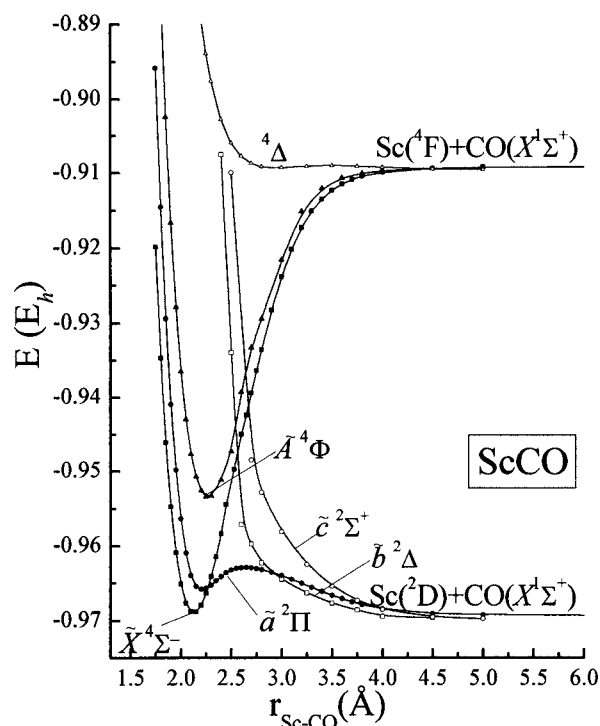


FIG. 1. RCCSD(T) Sc-CO potential energy profiles of $\tilde{X}^4\Sigma^-$, $\tilde{A}^4\Phi$, $\tilde{a}^2\Pi$, $\tilde{b}^2\Delta$, $\tilde{c}^2\Sigma^+$, and $^4\Delta$ states. All energies are shifted by +872 E_h .

C-RCCSD(T) level, but unfortunately the $^4\Pi$ cannot be calculated via the CC-theory, so we rely on the MRCI+Q results. The Sc-CO bond length increase is in complete conformity with conclusion (c) of Sec. II, which is also the cause of the slight ScC-O lengthening with respect to the free CO

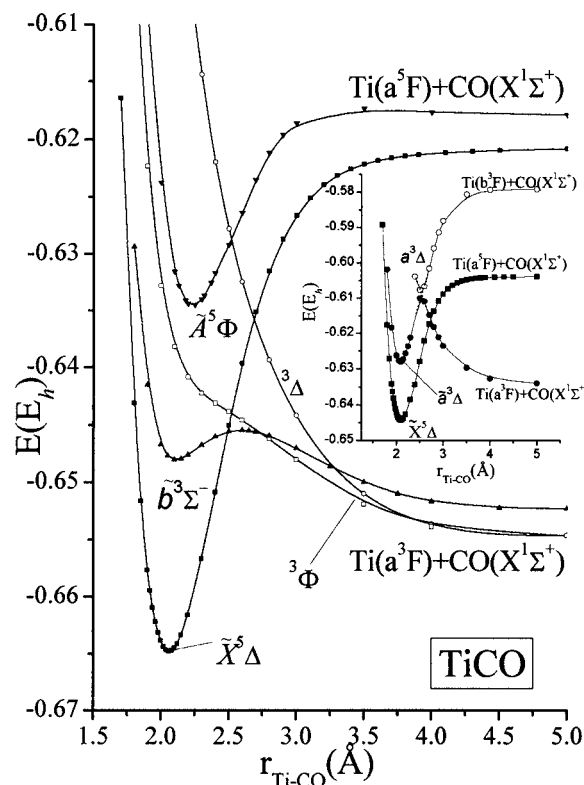
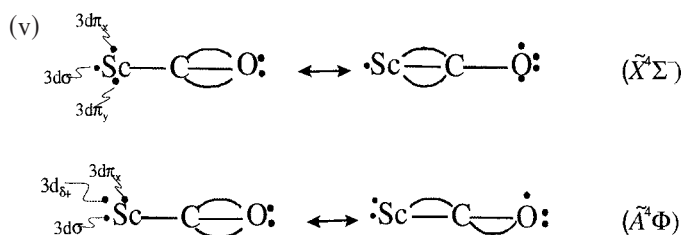


FIG. 2. RCCSD(T) Ti-CO potential energy profiles of $\tilde{X}^5\Delta$, $\tilde{b}^3\Sigma^-$, $\tilde{A}^5\Phi$, $^3\Phi$, and $^4\Delta$ states. The inset refers to ACPF potential curves of $\tilde{X}^5\Delta$ and $\tilde{a}^3\Delta$ states. All energies are shifted by +961 E_h .

in the three bound quartet ScCO states, being more pronounced in the $\tilde{X}^4\Sigma^-$ state; observation (d) of Sec. II. In other words both effects can be rationalized by the “resonance” structures (v). See also Schemes (ii), (iii), and (iv).



Finally we would like to make some comments on the dipole moment. According to the level of calculation and the technique, i.e., expectation value ($\langle\mu\rangle$) or finite field (μ_{FF}), the value of the $\tilde{X}^4\Sigma^-$ dipole moment varies from 2.0 to 3.4 D. Trusting more the μ_{FF} values³¹ and the CC-approach because the system is of single reference character along the whole Sc-CO PEC (*vide supra*), the recommended μ value of $\tilde{X}^4\Sigma^-$ state is -3.4 D referring to a Sc^+-CO^- polarity.

We turn now to the quartets $^4\Phi$, $^4\Pi$, and $^4\Delta$. As was discussed in Sec. II the $^4\Delta$ state correlates to $\text{Sc}(^4F; M_L = \pm 2) + \text{CO}$ and is, indeed, repulsive as expected (Fig. 1).

The next bound quartet state is of Φ spatial symmetry with a binding energy $D_e = 27.2(28.8)[26.6]$ kcal/mol with respect to $\text{Sc}(^4F) + \text{CO}(X^1\Sigma^+)$ at the RCCSD(T) (C-RCCSD(T)) [C-RCCSD(T)+relativity] level. Corresponding values at the MRCI, MRCI+Q, or ACPF level are smaller by about 4–5 kcal/mol because of mixed correlation-size non-extensivity effects (see Table III). The MRCI equilibrium atomic Mulliken populations given below, as well as the binding mechanism and the relative position of the $\tilde{A}^4\Phi$ with respect to the other quartet states, are in harmony with the thoughts expressed in Sec. II,

$$4s^{0.88}3d_{z^2}^{0.13}4p_z^{0.27}4p_x^{0.10}4p_y^{0.10}3d_{xz}^{0.13}3d_{yz}^{0.13}3d_{\delta^+}^{0.5}3d_{\delta^-}^{0.5}/_{Sc}2s^{1.44}2p_z^{0.98}2p_x^{0.72}2p_y^{0.72}3d_{xz}^{0.05}3d_{yz}^{0.05}/_C2s^{1.77}2p_z^{1.42}2p_x^{1.47}2p_y^{1.47}3d^{0.06}/_O$$

The comparison with the populations of the free CO reported previously shows clearly that $0.30 e^-$ are transferred from the $(2s2p_z)^{2.75}$ hybrid (free CO), to the $(4s3d_z2p_z)^{1.28}$ hybrid on Sc. The populations of the oxygen atom remain practically intact. However, through the π -system $1.0-2*(0.10+0.13) = 0.54 e^-$ migrate mainly to the p_π orbitals of the C atom. The net electron distribution in the $\tilde{A}^4\Phi$ state of ScCO is $Sc^{+0.22}_C^{-0.03}_O^{-0.19}$, very similar to the one of the $\tilde{X}^4\Sigma^-$ state (*vide supra*).

Depending on the method the $\tilde{A}^4\Phi \leftarrow \tilde{X}^4\Sigma^-$ energy separation (T_e) ranges from an unacceptable 788 cm^{-1} value (MRCI) to 3932 cm^{-1} (C-RCCSD(T)). Observe though the substantial improvement of T_e at the MRCI+Q level in comparison to the other methods. The relatively good agreement among the size extensive methodologies listed in Table III suggests that $T_e(\tilde{A}^4\Phi \leftarrow \tilde{X}^4\Sigma^-) \approx 4000 \text{ cm}^{-1}$.

Because the character of the $\tilde{A}^4\Phi$ state can be considered as adequately described by a single reference configuration [see Eq. (4)], the recommended dipole moment value is 2.7 D. The rather low ACPF $\mu_{FF} = 2.19$ D can be attributed to the vagaries of the ACPF *ad hoc* energy functional.

As discussed in Sec. II the $^4\Pi$ state is “chemically” very similar to the $\tilde{A}^4\Phi$ state, but the multireference character of the $^4F M_L = \pm 1$ component of the Sc atom [Eq. (2)], invalidates a single reference description. Therefore, within a mul-

tireference description be it MRCI, MRCI+Q or ACPF, the $^4\Pi$ state is located about 1000 cm^{-1} above the \tilde{A} -state. Atomic MRCI populations, bonding and even dipole moment ($\mu_{FF} \approx 2.7-2.8$ D), are practically identical to the $\tilde{A}^4\Phi$ state. Finally, contrasting our CC and multireference calculations in the $\tilde{A}^4\Phi$ and our multireference results in the $\tilde{B}^4\Pi$ state, it is fair to say that within the accuracy of our approximations the \tilde{A} and \tilde{B} quartets are degenerate and of course with similar binding energies. The experimental $T_e(\tilde{B}^4\Pi \leftarrow \tilde{X}^4\Sigma^-)$ of Van Zee and Weltner³ of 500 cm^{-1} is certainly underestimated.

B. TiCO

The presence of the CO molecule lifts the four degenerate $M_L = 0, \pm 1, \pm 2, \pm 3$ vectors of the ground $^3F(4s^23d^2)$ atomic state of Ti, giving rise to four molecular triplets $^3\Sigma^-, ^3\Pi, ^3\Delta$, and $^3\Phi$, respectively. According to the discussion in Sec. II all these states should be repulsive because of the $4s^2$ distribution on Ti, and indeed they are. Figure 2 shows repulsive RCCSD(T) PECs of the $^3\Sigma^-, ^3\Delta$, and $^3\Phi$ states. The $^3\Pi$ state is not accessible at the single reference

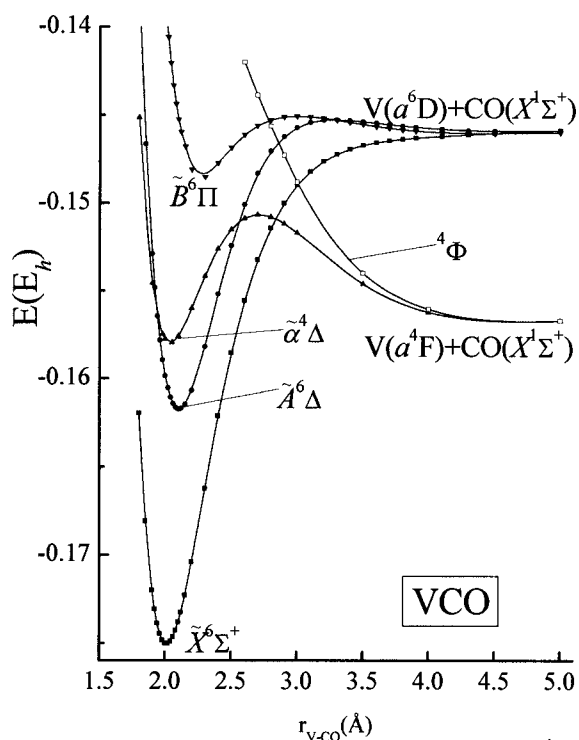


FIG. 3. RCCSD(T) V-CO potential energy profiles of $\tilde{X}^6\Sigma^+, \tilde{A}^6\Delta, \tilde{B}^6\Pi, \tilde{a}^4\Delta$, and $^4\Phi$ states. All energies are shifted by $+1056 E_h$.

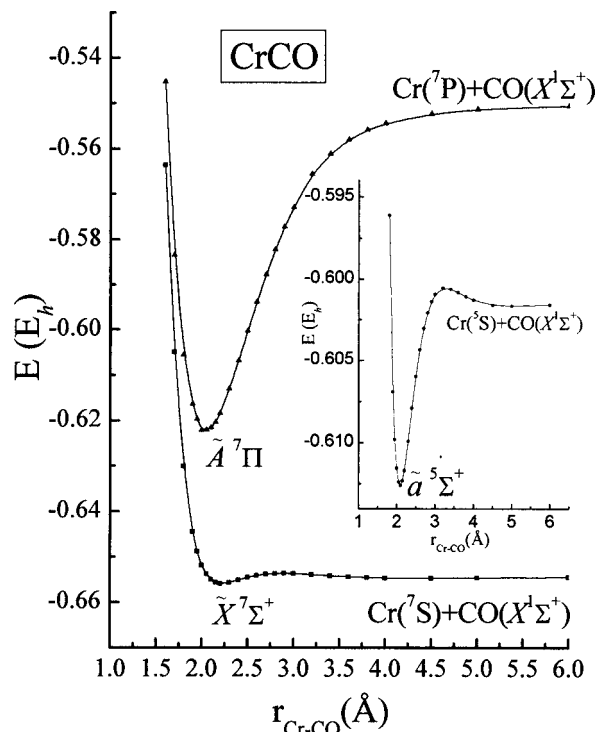


FIG. 4. RCCSD(T) Cr-CO potential energy profiles of $\tilde{X}^7\Sigma^+$ and $\tilde{A}^7\Pi$ states. The inset refers to MRCI+Q potential curve of $\tilde{a}^5\Sigma^+$ state. All energies are shifted by $+1156 E_h$.

CC-level, but its calculation at the MRCI(+Q) or ACPF level of theory proved that it is repulsive as well. The hump of the $^3\Sigma^-$ state and the shallow minimum that follows at $r_{\text{Ti-CO}} = 2.6$ and 2.1 Å, respectively, are completely analogous to the barrier and minimum of the $^2\Pi$ state of ScCO (*vide supra*). The barrier's height from the bottom of the well is about 2 kcal/mol.

We would like now to comment on the $^3\Delta$ state: Although it looks repulsive at the RCCSD(T) single reference level (Fig. 2), in “reality” it is bound because of an avoided crossing with another $^3\Delta$ state correlating to the fifth $b^3F(4\bar{5}^13d^3)$ excited state of Ti, located $11\,450.3$ cm^{-1} above its ground a^3F state.²² The situation is succinctly displayed in the inset of Fig. 2, where the PECs of the two $^3\Delta$ states have been computed at the ACPF level; the $\tilde{X}^5\Delta$ ACPF PEC is also shown for reasons of comparison. We conclude that the $^3\Delta$ state is the first excited state of TiCO with $T_e = 3\,757(3\,254)[3\,554]\text{cm}^{-1}$ at the MRCI (MCRI+Q) [ACPF] level (see Table III). It is important to say at this point that the crucial for the relative position of the $\tilde{a}^3\Delta$ state $\text{Ti}(b^3F \leftarrow a^3F)$ splitting, is calculated to be $11\,718$ ($11\,615$) [$12\,012$] cm^{-1} , in very good agreement with experiment.²²

With respect to $\text{Ti}(b^3F) + \text{CO}(X^1\Sigma^+)$ fragments we obtain $D_e = 25.3(28.3)[30.6]$ kcal/mol, with corresponding Ti–CO bond distances 2.068 (2.057) [2.088] Å at the MRCI (MRCI+Q) [ACPF] approximations, very similar to the $\tilde{X}^5\Delta$ Ti–CO bond length as expected (see Table III). Obviously the bonding mechanism of the $\tilde{X}^5\Delta$ and $\tilde{a}^3\Delta$ states is identical, related to the similarity of the a^5F and b^3F Ti configurations (see below). It is fair to say that Barnes and Bauschlicher¹³ say clearly that the first excited state is of $^3\Delta$ symmetry, correlating to $\text{Ti}(b^3F)$ and with $T_e = 3629$ cm^{-1} , very similar to ours.

The quintet bound states, including the ground state, correlate to $\text{Ti}(a^5F; 4s^13d^3)$, 6500 cm^{-1} above the a^3F state.²² The MRCI (MCRI+Q) [ACPF] {RCCSD(T)} <C-RCCSD(T)> $a^5F \leftarrow a^3F$ splitting is 4209 (5686) [6608] [7435] < 5782 > cm^{-1} . The s^1d^3 $M_L = 0, \pm 1, \pm 2, \pm 3$ vectors are given in Eqs (5)–(8),

$$|0\rangle = \frac{\sqrt{4}}{\sqrt{5}}|4s^13d_\sigma^13d_{\delta+}^13d_{\delta-}^1\rangle - \frac{\sqrt{1}}{\sqrt{5}}|4s^13d_\sigma^13d\pi_x^13d\pi_y^1\rangle, \quad (5)$$

$$|\pm 1\rangle_{B_1} = \sqrt{\frac{4}{10}}|4s^13d\pi_y^13d_{\delta+}^13d_{\delta-}^1\rangle + \sqrt{\frac{3}{10}}|4s^13d_\sigma^13d\pi_x^13d\delta_+^1\rangle + \sqrt{\frac{3}{10}}|4s^13d_\sigma^13d\pi_y^13d_{\delta-}^1\rangle, \quad (6)$$

$$|\pm 2\rangle_{A_1} = |4s^13d\pi_x^13d\pi_y^13d_{\delta-}^1\rangle, \quad (7)$$

$$|\pm 3\rangle_{B_1} = \sqrt{\frac{5}{10}}|4s^13d_\sigma^13d\pi_x^13d_{\delta+}^1\rangle + \sqrt{\frac{5}{10}}|4s^13d_\sigma^13d\pi_y^13d_{\delta-}^1\rangle. \quad (8)$$

The linear interaction of CO with the 5F state of Ti results to $^5\Sigma^-$, $^5\Pi$, $^5\Delta$, and $^5\Phi$ molecular states, respectively. In the spirit of Sec. II the expected ordering of quintets is $\tilde{X}^5\Delta < ^5\Pi \approx ^5\Phi < ^5\Sigma^-$ with Ti–CO bonding mechanisms similar to those of the ScCO case. Observe also that the $\tilde{X}^5\Delta$ TiCO state is of single reference character, so it can be well described within the RCCSD(T) formalism.

At the MRCI level the $\tilde{X}^5\Delta$ state of TiCO is satisfactorily described by a single reference function, $|\tilde{X}^5\Delta\rangle_{A_2} \approx 0.94|1\sigma^22\sigma^23\sigma^21\pi_x^21\pi_y^24\sigma^12\pi_x^12\pi_y^11\delta_+^1\rangle$, with the following MRCI atomic equilibrium populations

$$4s^{0.85}3d_z^{0.12}4p_z^{0.27}4p^{0.05}3d_{xz}^{0.82}3d_{yz}^{0.82}3d_{\delta+}^{1.0} / \text{Ti} 2s^{1.50}2p_z^{0.98}2p_x^{0.61}2p_y^{0.61}3d_{xz}^{0.06}3d_{yz}^{0.06} / \text{C} 2s^{1.77}2p_z^{1.42}2p_x^{1.44}2p_y^{1.44}3d^{0.06} / \text{O}$$

Apart from the $3d_{\delta+}^{1.0}$ “observer” electron, the remaining distributions are practically the same with those of the $\tilde{X}^4\Sigma^-$ state of ScCO, suggesting the same binding mode; see also Schemes (ii) and (iii). The net charge redistribution is $\text{Ti}^{+0.05}\text{-C}^{+0.09}\text{-O}^{-0.14}$. The binding energy with respect to $\text{Ti}(^5F) + \text{CO}$ at the RCCSD(T) (C-RCCSD(T)) [C-RCCSD(T)+DKH] level is 27.5 (29.5) [27.7] kcal/mol, or $D_0 = D_e - \text{ZPE}(\text{RCCSD(T)}) = 26.6$ kcal/mol (Table III). The corresponding multireference D_e values are significantly smaller but they converge consistently to a 27 kcal/mol value as we move from MRCI to MRCI+Q to ACPF.

As in the case of the $\tilde{X}^4\Sigma^-$ state of ScCO, the Ti–CO bond distance increases significantly, 0.15 – 0.17 Å from the $\tilde{X}^5\Delta$ to $\tilde{A}^5\Phi$ and $\tilde{B}^5\Pi$ states in all methods of calculation, for reasons stated in Sec. II. Correspondingly, the RCCSD(T)

or C-RCCSD(T) TiC–O bond length of $\tilde{X}^5\Delta$ and $\tilde{A}^5\Phi$ states increases by about 0.03 and 0.02 Å with respect to the free CO, respectively.

Trusting our CC results we can claim that the dipole moment of $\tilde{X}^5\Delta$ is $\mu = -2.4$ D with $\text{Ti}^+ - \text{CO}^-$ polarity. Observe though the catastrophic MRCI $\langle \mu \rangle = +0.27$ D value, as compared to the significantly improved MRCI (MRCI+Q) $\mu_{\text{FF}} = -0.92$ (-1.73) D values relative to the CC result.

According to Table III the next quintet is of Φ symmetry about 20 kcal/mol above the $\tilde{X}^5\Delta$ state at the C-RCCSD(T)+DKH level. At the same level, $D_e(D_0) = 7.1$ (6.4) kcal/mol with respect to $\text{Ti}(^5F) + \text{CO}$. At the MRCI+Q or ACPF approaches D_e values are 1 to 2 kcal/mol smaller. The binding of $\tilde{A}^5\Phi$ is very similar to that of ScCO $\tilde{A}^4\Phi$, albeit by about 20 kcal/mol smaller due

to the presence of the d_{σ}^1 density in the case of TiCO. The total MRCI Mulliken electron distribution is $\text{Ti}^{+0.17}\text{-C}^{-0.02}\text{-O}^{-0.15}$.

At the RCCSD(T) level we were unable to obtain the dipole moment (μ_{FF}) of the $\tilde{A}^5\Phi$ state, because of wild energy fluctuations in the presence of the external electric field. As we can see in Table III, depending on the multireference method, dipole moments differ substantially indicating the difficulty of obtaining reliable electric moments for such systems.³¹

At the ACPF and MRCI+Q level the $\tilde{B}^5\Pi$ state of TiCO is bound by less than 5 kcal/mol, located 2.8 kcal/mol above the $\tilde{A}^5\Phi$ state. The $^5\Sigma^-$ state although unbound at the MRCI+Q level shows a shallow minimum while is slightly bound at the ACPF level with $D_e \approx 4.5$ kcal/mol. Notice that the $\tilde{B}^5\Pi$ and the $\tilde{C}^5\Sigma^-$ states are practically degenerate.

C. VCO

The ground state distribution $4s^23d^3(a^4F)$ of the V atom implies VCO $^4\Sigma^-$, $^4\Pi$, $^4\Delta$, and $^4\Phi$ states of repulsive character. Figure 3 shows the repulsive potential curve of the $^4\Phi$ state at the RCCSD(T) level. The $^4\Sigma^-$ and $^4\Pi$ states, inaccessible through the CCSD(T) approach, were calculated at the MRCI(+Q) level and proved unbound as well.

The RCCSD(T) PEC of $^4\Delta$ shown in Fig. 3 is more interesting: It presents a hump at a V–CO distance of 2.7 Å caused by the $4s^2$ V electron distribution, followed by a well the depth of which is 4.8 kcal/mol with respect to the barrier's maximum and 0.8 kcal/mol lower with respect to the

end products. The situation is completely analogous to the $^2\Pi$ and $^3\Sigma^-$ states of ScCO and TiCO, respectively (*vide supra*).

Bound VCO sextets are expected from the first excited state of V atom, $^6D(4s^13d^4)$, 1977.3 cm^{-1} (=5.65 kcal/mol) above the a^4F term. The $M_L=0, \pm 1$, and ± 2 vectors shown below give rise to $^6\Sigma^+$, $^6\Pi$, and $^6\Delta$ molecular states, respectively,

$$|0\rangle_{A_1} = |4s^13d\pi_x^13d\pi_y^13d_{\delta+}^13d_{\delta-}^1\rangle, \quad (9)$$

$$|\pm 1\rangle_{B_2} = |4s^13d_{\sigma}^13d\pi_x^13d_{\delta+}^13d_{\delta-}^1\rangle, \quad (10)$$

$$|\pm 2\rangle_{A_1} = |4s^13d_{\sigma}^13d\pi_x^13d\pi_y^13d_{\delta-}^1\rangle. \quad (11)$$

From Eqs. (9)–(11) it is clear that the most bound of the sextets should be of Σ^+ spatial symmetry (does not include the $3d_{\sigma}^1$ orbital while including the $3d\pi_x^1$ and $3d\pi_y^1$ orbitals), followed by the $^6\Delta$ and $^6\Pi$ states. This ordering is confirmed by the RCCSD(T) PECs shown in Fig. 3, $\tilde{X}^6\Sigma^+ < \tilde{A}^6\Delta < \tilde{B}^6\Pi$. In essence, the single reference character of these states renders our CC calculations reliable enough.

From Table III we see that the binding energy of the $\tilde{X}^6\Sigma^+$ state is $D_e(D_0)=19.3(18.2)$ kcal/mol at the C-RCCSD(T)+DKH level using the RCCSD(T) ZPE of 1.1 kcal/mol. Observe the really deplorable MRCI or MRCI+Q D_e values and the very long V–CO distances as compared to the CC results. The MRCI equilibrium atomic populations are as follows:

$$4s^{0.90}3d_{z^2}^{0.09}4p_z^{0.22}3d_{xz}^{0.92}3d_{yz}^{0.92}3d_{\delta+}^{1.0}3d_{\delta-}^{1.0} / \sqrt{2} s^{1.53} 2p_z^{0.99} 2p_x^{0.57} 2p_y^{0.57} 3d_{xz}^{0.06} 3d_{yz}^{0.06} / c 2s^{1.76} 2p_z^{1.42} 2p_x^{1.42} 2p_y^{1.42} / o$$

In total, about 0.22 e^- are transferred through the σ -frame to the V atom, while 0.16 e^- are moving back via the π route to the –CO moiety. Notwithstanding the pitfalls of Mulliken analysis it is interesting that the metal appears slightly negative: $\text{V}^{-0.08}\text{-C}^{+0.16}\text{-O}^{-0.08}$. The binding mechanism remains the same as in the ScCO ($\tilde{X}^4\Sigma^-$) and TiCO ($\tilde{X}^5\Delta$) species, but with a considerable smaller electron back transfer through the π -skeleton from the metal to CO. Indeed, while the σ -transfer from CO to M (=Sc, Ti, V) remains practically the same, the back transfer decreases from about 0.50 to 0.26 to 0.16 e^- from ScCO to TiCO to VCO, respectively.

Now the dipole moment of the $\tilde{X}^6\Sigma^+$ state of VCO shows remarkable fluctuations depending on the calculational approach, ranging from –1.94 to +2.23 D (see Table III). Being aware that our MRCI wave function suffers from severe nonextensivity effects, we performed MRCI calcula-

tions but using the C-RCCSD(T) geometry, i.e., $r_{\text{M-CO}}=2.00$ Å, $r_{\text{MC-O}}=1.15$ Å. The total MRCI (MRCI+Q) energy increased by 4.6(1.4) mE_h, the atomic populations changed but only slightly resulting to a total charge distribution of $\text{V}^{-0.03}\text{-C}^{+0.17}\text{-O}^{-0.14}$, but the dipole moment changed dramatically: $\langle \mu(\text{MRCI}) \rangle / \mu_{\text{FF}}(\text{MRCI}) / \mu_{\text{FF}}(\text{MRCI+Q}) = +1.32 / +0.31 / -0.25$ D, respectively. Assuming that the $\mu_{\text{FF}}[\text{C-RCCSD(T)}] = -1.8$ D value is the most reliable, we see that the multireference +1.32, +0.31, –0.25 D sequence is, at least, going towards the correct direction.

The potential energy profiles of the $\tilde{A}^6\Delta$ and $\tilde{B}^6\Pi$ states are shown in Fig. 3. The C-RCCSD(T) binding energy of the $\tilde{A}^6\Delta$ with respect to $\text{V}(a^6D)+\text{CO}$ is $D_e=11.3$ kcal/mol, but this of the $\tilde{B}^6\Pi$ state is just 3.3 kcal/mol with $T_e(\tilde{B}^6\Pi \leftarrow \tilde{A}^6\Delta)=2830$ cm^{-1} (=8 kcal/mol). Observe that at the MRCI level the $\tilde{A}^6\Delta$ state is practically unbound and that the

sign of the dipole moment suggests that its *negative* end is on the metal atom.

D. CrCO

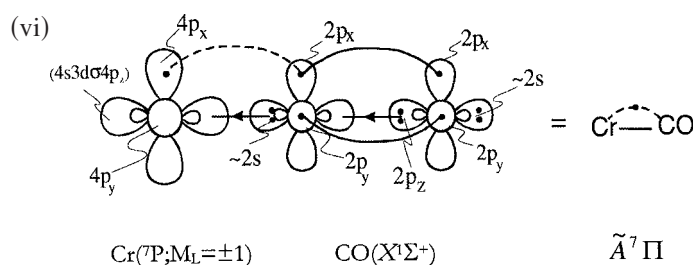
A single molecular CrCO state originates from the ground ${}^7S(4s^13d^5)$ state of the Cr atom, obviously of ${}^7\Sigma^+$ symmetry if linear. Complete geometry optimization at the RCCSD(T) level indicates that the molecule is bent ($\angle\text{CrCO}=154^\circ$), therefore of ${}^7A'$ symmetry and a “binding” energy of 1.06 kcal/mol. The barrier to linearity is 75 cm^{-1} . At the same CrCO angle, but optimizing only the two bond distances we get $D_e=3.72\text{ kcal/mol}$ at the C-RCCSD(T) level. Finally, adding the DKH relativistic effects and using the C-RCCSD(T) distances of the linear geometry, $D_e=2.1\text{ kcal/mol}$, as compared to an experimental value of less than 1.5 kcal/mol.⁸ The PEC of the linear CO approach to the 7S of Cr(${}^7\Sigma^+$) is shown in Fig. 4.

The first excited state of CrCO correlates to Cr(${}^5S;4s^13d^5$), it is of ${}^5\Sigma^+$ symmetry, and has a binding energy of 5 to 10 kcal/mol depending on the method of calcu-

lation. It should be mentioned that this is a genuine multireference state and is completely inaccessible through a single reference method. Giving more weight to the ACPF and C-MRCI+Q methods, the recommended D_e value is about 10 kcal/mol with $\mu_{\text{FF}}\approx+2.5\text{ D}$; its MRCI+Q PEC is given in the inset of Fig. 4.

Our last calculated state is of ${}^7\Pi$ symmetry, “strongly” bound, but with respect to the sixth excited state of Cr, $z^7P(3d^54p^1)$, experimentally²² [(RCCSD(T) calculated] 23 415 [22 895] cm^{-1} above the ground 7S state. The C-RCCSD(T) (C-MRCI+Q) binding energy is 48.4(38.3) kcal/mol at $r_{\text{Cr-CO}}=1.990(1.933)\text{ \AA}$. This much larger D_e value of the $\tilde{A}^7\Pi$ state relative to all other M-CO calculated binding energy values, is the result of the available $4p_z$ empty orbital and its ability to hybridize with the $4s$ Cr orbital function. The vBL diagram (vi) captures the essence of the binding process, while suppressing the five $3d$ half-occupied Cr orbitals.

The MRCI equilibrium atomic populations completely support Scheme (vi):



$$4s^{0.77}3d_{z^2}^{0.45}4p_z^{0.14}4p_x^{0.52}3d_{xz}^{1.0}3d_{yz}^{0.97}3d_{\delta+}^{1.0}3d_{\delta-}^{1.0} / \text{Cr} 2s^{1.41}2p_z^{0.96}2p_x^{0.88}2p_y^{0.56}3d_{\pi}^{0.10} / \text{C} 2s^{1.76}2p_z^{1.42}2p_x^{1.52}2p_y^{1.39}3d^{0.06} / \text{O}$$

Observe first that upon bonding the $3d_{xz}, 3d_{yz}, 3d_{\delta+}$, and $3d_{\delta-}$ metal orbitals remain intact. The $4s3d_{z^2}4p_z$ hybrid hosts $0.77+0.45+0.14=1.36\text{ e}^-$, 0.36 more from infinity ($3d_{z^2}=1.0$), removed from the σ -frame of CO. Concomitantly, 0.5 e^- are back-transferred from the $4p_x$ Cr orbital ($4p_x=1.0$ at infinity) to the π -system of CO. The net polarity of the molecule appears to be $\text{Cr}^{+0.13}\text{-C}^{+0.03}\text{-O}^{-0.16}$.

The C-RCCSD(T) dipole moment is $\mu_{\text{FF}}=-3.9\text{ D}$, but it is remarkable that $\langle\mu\rangle/\mu_{\text{FF}}=-2.8/-5.8\text{ D}$ at the MRCI or C-MRCI level.³¹ We dare to recommend a dipole moment of about -4.5 D for the $\tilde{A}^7\Pi$ state of CrCO.

V. CONCLUSIONS

We examined by coupled-cluster (RCCSD(T)) and multireference (MRCI=CASSCF+1+2) methods the ground and few low-lying excited states of the MCO series, where M=Sc, Ti, V, and Cr. For almost all states we report M-CO potential energy curves at the RCCSD(T)/ANO+AQZ level. Our conclusions can be codified as follows.

- (1) The ground states of ScCO, TiCO, VCO, and CrCO are ${}^4\Sigma^-, {}^5\Delta, {}^6\Sigma^+$, and ${}^7A'({}^7\Sigma^+)$, respectively; with the exception of the \tilde{X}^7A' state, they correlate to the first excited state of the M atom.

TABLE IV. Ground state “best” estimates of dissociation energies (D_0), equilibrium bond lengths ($r_{\text{M-CO}}$) and dipole moments (μ) of ScCO ($\tilde{X}^4\Sigma^-$), TiCO ($\tilde{X}^5\Delta$), VCO ($\tilde{X}^6\Sigma^+$) and CrCO (\tilde{X}^7A'). In parentheses results from the literature.^a

Species	D_0 (kcal/mol)	$r_{\text{M-CO}}$ (\AA)	μ (Debye)
ScCO	36 (29.7)	2.080 (2.076)	-3.4 (-3.41)
TiCO	27 (35.5)	2.033 (2.016)	-2.4 (-3.08)
VCO	18 (33.0)	2.00 (1.969)	-1.8 (-3.06)
CrCO	2 (9.0)	2.18 (2.156)	(-0.87)
	[<1.5] ^b		

^aDFT (BPW91)/[6-311+G*], Ref. 17.

^bExperimental value, Ref. 8.

- (2) Table IV summarizes our estimates of dissociation energies $D_0(=D_e-ZPE)$, dipole moments and M–CO bond lengths of the four ground MCO states along with recent DFT (BPW91) results from Ref. 17 of Gutsev *et al.* Although the DFT and *ab initio* r_{M-CO} bond distances are in acceptable agreement, the DFT fails completely in reproducing the *ab initio* M–CO dissociation energies, i.e., the trend of about 10 kcal/mol decrease from ScCO to TiCO to VCO, at both the CC and MRCI+Q level. The situation becomes worse in CrCO where the system is practically unbound, but the DFT predicts a 9 kcal/mol binding energy.
- (3) Our results are in good agreement with the few experimental data available, namely, stretching MC–O frequencies and the Cr···CO van der Waals-type interaction in the \tilde{X}^7A' state.
- (4) The bonding can be attributed to a relatively modest and practically of the same magnitude σ -charge transfer from CO to the metal along the ScCO, TiCO, and VCO series, and a stronger back π -donation from the metal atoms to –CO due to “conjugation.” However, this conjugation effect diminishes from ScCO to CrCO because the 3d-orbitals of the metal become less available for interaction with the p_π orbitals of CO as we move from Sc to Cr. This is also the reason of the 10 kcal/mol sequential decrease in binding energy reported above (Table IV).
- (5) It is our opinion that the bonding in these monocarbonyl systems is rather atypical, meaning that cannot easily be classified. Perhaps it is more realistic to speak of van der Waals-polarization interactions most pronounced in the $\tilde{X}^4\Sigma^-$ state of ScCO and vanishing almost completely in the CrCO \tilde{X}^7A' state.

ACKNOWLEDGEMENTS

C. Koukounas and S. Kardahakis express their gratitude to the Hellenic State Scholarship Foundation (IKY) for financial support. A. Mavridis is grateful to the EPEAEK program PYTHAGORAS (Grant No. 70/3/7373) for basic research.

¹M. Zhou, L. Andrews, and C. W. Bauschlicher, Jr., Chem. Rev. (Washington, D.C.) **101**, 1931 (2001), and references therein.

- ²S. B. H. Bach, C. A. Taylor, R. J. Van Zee, M. T. Vala, and W. Weltner, Jr., J. Am. Chem. Soc. **108**, 7104 (1986).
- ³R. J. Van Zee and W. Weltner, Jr., J. Am. Chem. Soc. **111**, 4519 (1989).
- ⁴M. Zhou and L. Andrews, J. Phys. Chem. A **103**, 2964 (1999).
- ⁵M. J. McQuaid, K. Morris, and J. L. Gole, J. Am. Chem. Soc. **110**, 5280 (1988).
- ⁶M. Zhou and L. Andrews, J. Phys. Chem. A **103**, 5259 (1999).
- ⁷R. J. Van Zee, S. B. H. Bach, and W. Weltner, Jr., J. Phys. Chem. **90**, 583 (1986).
- ⁸S. A. Trushin, K. Sugawara, and H. Takeo, Chem. Phys. Lett. **267**, 573 (1997).
- ⁹P. F. Souter and L. Andrews, J. Am. Chem. Soc. **119**, 7350 (1997).
- ¹⁰L. Andrews, M. Zhou, G. L. Gutsev, and X. Wang, J. Phys. Chem. A **107**, 561 (2003).
- ¹¹G. H. Jeung and J. Koutecky, Chem. Phys. Lett. **129**, 569 (1986).
- ¹²R. F. Frey and E. R. Davidson, J. Chem. Phys. **90**, 5541 (1989); *ibid.* **90**, 5555 (1989).
- ¹³L. A. Barnes and C. W. Bauschlicher, Jr., J. Chem. Phys. **91**, 314 (1989).
- ¹⁴G. H. Jeung, J. Am. Chem. Soc. **114**, 3211 (1992).
- ¹⁵C. Adamo and F. Lejl, J. Chem. Phys. **103**, 10605 (1995).
- ¹⁶C. Adamo and F. Lejl, Chem. Phys. Lett. **246**, 463 (1995).
- ¹⁷G. L. Gutsev, L. Andrews, and C. W. Bauschlicher, Jr., Chem. Phys. **290**, 47 (2003).
- ¹⁸J. Pilme, B. Silvi, and M. E. Alikhani, J. Phys. Chem. A **107**, 4506 (2003).
- ¹⁹R. M. Sosa, P. Gardiol, and G. Beltrame, Int. J. Quantum Chem. **69**, 371 (1998).
- ²⁰R. Fournier, J. Chem. Phys. **98**, 8041 (1993).
- ²¹M. J. S. Dewar, Bull. Soc. Chim. Fr. **18**, C71 (1951); J. Chatt and L. A. Duncanson, J. Chem. Soc. **1953**, 2939.
- ²²C. A. Moore, *Atomic Energy Levels*, NRSDS-NBS, Circular No 35, U.S. GPO, Washington DC, 1971.
- ²³K. P. Huber and G. Herzberg, *Constants of Diatomic Molecules* (Van Nostrand Reinhold, New York, 1979).
- ²⁴A. Kalemios, A. Mavridis, and J. F. Harrison, J. Phys. Chem. A **105**, 755 (2001); A. Kalemios and A. Mavridis, *ibid.* **106**, 3905 (2002); A. Kalemios, T. H. Dunning, Jr., and A. Mavridis, J. Chem. Phys. **123**, 14301 (2005); *ibid.* **123**, 14302, (2005).
- ²⁵C. W. Bauschlicher, Jr., Theor. Chim. Acta **92**, 183 (1995).
- ²⁶T. H. Dunning, Jr., J. Chem. Phys. **90**, 1007 (1989); R. A. Kendall, T. H. Dunning, Jr., and R. J. Harrison, *ibid.* **96**, 6796 (1992).
- ²⁷M. Douglas and N. M. Kroll, Ann. Phys. (N.Y.) **82**, 89 (1974); B. A. Hess, Phys. Rev. A **32**, 756 (1985); B. A. Hess, *ibid.* **33**, 3742 (1986).
- ²⁸R. J. Gdanitz and R. Ahlrichs, Chem. Phys. Lett. **143**, 413 (1988); H.-J. Werner and P. J. Knowles, Theor. Chim. Acta **84**, 95 (1992).
- ²⁹R. D. Amos, A. Bernhardsson, A. Berning *et al.*, MOLPRO 2000 is a package of *ab initio* programs designed by H.-J. Werner and P. J. Knowles, version 2002.6.
- ³⁰J. F. Stanton, J. Gauss, J. D. Watts *et al.* ACES II is a program product of the Quantum Theory Project, University of Florida. Integral packages included are VMOL (J. Almlöf and R. Taylor. VPROPS; R. Taylor; ABACUS (T. Helgaker, H. J. Aa. Jensen, P. Jørgensen, J. Olsen, and P. R. Taylor).
- ³¹D. Tzeli and A. Mavridis, J. Chem. Phys. **118**, 4984 (2003); **122**, 056101 (2005).